ACS APPLIED MATERIALS & INTERFACES

Energy, Environmental, and Catalysis Applications

A Metal-Polydopamine Framework (MPDA) as an Effective Fluorescent Quencher for Highly Sensitive Detection of Hg (II) And Ag (I) ions Through Exonuclease III Activity

Ayyanu Ravikumar, Perumal Panneerselvam, and Norhashimah Morad

ACS Appl. Mater. Interfaces, **Just Accepted Manuscript** • DOI: 10.1021/acsami.8b05041 • Publication Date (Web): 24 May 2018

ACS Publications

is published by the American Chemical Society. 1155 Sixteenth Street N.W., Washington, DC 20036

A Metal-Polydopamine Framework (MPDA) as an Effective Fluorescent Quencher for Highly Sensitive Detection of Hg (II) And Ag (I) ions Through Exonuclease III Activity

Ayyanu Ravikumar[1], Perumal Panneerselvam[1]*, Norhashimah Morad[2]

[1]Department of Chemistry, SRM Institute of Science and Technology, Kattankulathur- 603 203, Tamil Nadu, India.

[2] Environmental Technology Division, School of Industrial Technology, University Sains Malaysia, 11800 Minden, Penang, Malaysia

* Corresponding author & E-mail address: panneerselvam.pe@ktr.srmuniv.ac.in

panneerchem82@gmail.comTel: +91 9688538842

Abstract

In this paper, we propose a metal-polydopamine framework (MPDA) with specific molecular probe which appears to be the most promising approach to a strong fluorescence quencher. The MPDA framework quenching ability towards various organic fluorophore such as aminoethylcomarin acetate (AMCA), 6-carboxyfluorescein (FAM), carboxyteramethylrhodamine (TAMRA) and Cy5 are used to establish a fluorescent biosensor that can selectively recognize Hg^{2+} and Ag^{+} ion. The fluorescent quenching efficiency was sufficient to achieve more than 96%. The MPDA framework also exhibits different affinities with ssDNA and dsDNA. In addition, the FAM labelled ssDNA was adsorbed onto MPDA framework, based on their interaction with the complex formed between MPDA frameworks/ssDNA taken as a sensing platform. By taking advantage of this sensor highly sensitive and selective determination of $Hg^{2+}$and Ag^{+} ions is achieved through Exonuclease III signal amplification activity. The detection limits of $Hg^{2+}$and Ag^{+} achieved to be 1.2 pM and 34 pM respectively, were compared to co-existing metal ions and GO based sensors. Furthermore, the potential applications of this study establish the highly sensitive fluorescence detection targets in environmental and biological fields.

Keywords: Metal-polydopamine frameworks, Exonuclease III, mercury, silver, ssDNA

1. INTRODUCTION

Heavy metal contamination is a serious global problem because it is very deleterious to human health and the environment owing to their accumulation in the food chain as non-biodegradable pollutants is persistence in nature. Among them known toxic metal, Hg^{2+} and Ag^{+} ions are the one of the most prevalent environmental water pollutants with persistent bioaccumulation and high toxicity.[1-4] Even at invisible trace levels of Hg^{2+} ion serious damage to the health problems such as brain damage, kidney failure, nervous disorder and even death may occur.[5, 6] In addition, Ag^{+} ions are detrimental to human health due to highly toxic and can lead to variety of unpleasant health effects. Therefore, the effective detection of trace amount of heavy metal ions concentration is important for environmental protection and health monitoring. Much effort has been made to develop the Hg^{2+} and Ag^{+} sensors, including atomic adsorption spectroscopy (AAS), inductively coupled plasma mass spectroscopy (ICP-MS), inductively coupled plasma atomic emission spectroscopy (ICP-OES), cold vapour atomic fluorescence spectroscopy (CV-AFS) and cold vapour atomic adsorption spectroscopy (CV-AAS).[7-12] These widely used instrumental analytical techniques have some limitations, including expensive equipments, complication in sample preparation and requires well-trained person. To defeat this problem, the large number of well-designed sensors based on this T- Hg^{2+}-T and C-Ag^{+}-C coordination chemistry has been developed by fluorescent,[13,14] colorimetric[15,16] and electrochemical[17] sensing methods, of which sensitive and selective detection of Hg^{2+} and Ag^{+} ions by fluorescent methods is most competitive and have attracted great attention in recent years.

Recently, more interest has been shown in the development of nanomaterial based fluorescent bio sensor. In particular, this type of sensor based on fluorescent resonance energy transfer (FRET) mechanism which relies on the fluorescence quenching the fluorophore and quenching

materials.[18] These nano-quenching materials can efficiently quench fluorophore and eliminating the selection issue of fluorescence quencher pair, improving the signal to noise ratio of aptamer. So far, the large number of nanomaterials have been applied to the fluorescence sensing of metal ions including graphene oxide, carbon nitride, transition metal sulfide nanosheets and carbon nanotubes.[19-22] Although these nanomaterials have been successfully demonstrated by sensitive and specific fluorescence detection of metal ions, the preparation of these nanomaterials is not easy and there is difficulty in uniform dispersion and some of these nanomaterials are toxic. Therefore it can be anticipated that the searching of new nanomaterials is aggravated towards the replacement.

Over the past few decades, metal organic frame works (MOFs) is represented as excellent candidate of materials that have attracted for extensive research interest due to their high surface area, flexible porosity, tunable nature and morphology can be easily turned upon selection of different metal ions and organic bridging ligand have been developed as a new class of solid adsorbent. The nanoscale MOFs has the size dependant properties, if it is properly exploit we may expand their scope for numerous practical applications such as biomedicine, gas storage, catalysis, hydrogen storage, drug delivery and sensing.[23,24] Now a days, the MOFs have attracted considerable attention for the excellent biosensing platforms for detection of metal ions and biomolecules.[25] In the mean time, polydopamine is a type of bio-polymerized material with excellent biocompatibility and biodegradability.[26] The redox active and quinone structure of polydopamine enable its surface to coat on various material surfaces. In addition, the polydopamine is naturally provides excellent electron acceptor.[27] Therefore, MOFs with polydopamine as the sensing platform may improve the quenching efficiency and enhance the

sensitivity of fluorescence sensor efficiently. The resulting MOFs with polydopamine based fluorescence sensor for detection of metal ions has never been reported.

In this work, we explore the fluorescent quenching ability of metal polydopamine framework for high sensitive and selective detection of Hg^{2+} and Ag^{+} ions. Specifically, four different organic fluorophore have quenching efficiency including aminoethylcomarinacetate (AMCA), 6-carboxyfluorescein (FAM), carboxyteramethylrhodamine (TAMRA) and Cy5 were demonstrated. The FAM labeled ssDNA could absorb the metal polydopamine frameworks to form a stable complex. By taking advantage of this sensing platform for detection of mercury and silver ions assisted through Exonuclease III signal amplification strategy has not been reported yet. To the best of our knowledge, this is the first work on strong fluorescence quenching ability of various fluorescent dyes of metal polydopamine frameworks. This proposed assay can be further extended to other environmental and biological applications.

2. EXPERIMENTAL

2.1. Reagents

Cobalt nitrate hexahydrate, Zinc nitrate hexahydrate, 2-methylimidazole, dopamine hydrochloride, are purchased from Sigma-Aldrich. Ethanol, methanol, tris (hydroxymethyl) aminomethane are from Alfa Aesar. Exonuclease III was received from Thermo Fisher scientific (India). The stock solution of DNAs were prepared by using Tris buffer (20 mM Tris, 200 mM KCl, 10 mM $MgCl_2$, pH= 8.0). All the chemical reagents used in this experiment were of analytical grade and used directly without further purification. The DNA oligonuclotides were purchased from integrated DNA technologies (IDT, Avantor, India) and their DNA probes are given as follows.

P-AMCA: 5'-ACTGTCCCCTTGCAGT-AMCA-3'

P-Cy5: 5'-ACTGTCCCCTTGCAGT-Cy5-3'

P-TAMRA: 5'-ACTGTCCCCTTGCAGT-TAMRA-3'

P-FAM: 5'-ACTGTCCCCTTGCAGT-FAM-3'

P-T DNA: 5'-ATTGTTTTGTTTCCCCTTTCTTTTCTTT-FAM-3'

P- C DNA: 5'-ACCTGCCCCACCTTTTCCTCCCCCACCT-FAM-3'

2.2. Synthesis of ZIF-67

In a typical procedure, solutions of 1.455 g of Co $(NO_3)_2.6H_2O$ and 1.65 g of 2-methylimidazole were dissolved in 30 mL of methanol separately.[28] The resulting solutions were mixed and stirred for 3 h at room temperature. Finally, the reaction mixture was cooled down at room temperature and collected by centrifuge, by washed with deionized water and methanol and dried at 60 ºC overnight.

2.3. Synthesis of hollow metal–polydopamine framework

Generally, hollow metal-polydopamine frameworks (MPDA) was synthesized according to the following procedure.[29] In the synthesis at first a mixed solution was prepared with 20 ml of ethanol and 15 ml of water. To this solution 10 mg of ZIF-67 was uniformly dispersed under ultrasonication. Then dopamine (4 mg) was added into above solution with magnetic stirring. Then the resulting mixed solution under stirring for 5 min, after that 10 mL of aqueous solution of Tris (hydroxymethyl) aminoethane (20 mM, pH= 8.5) was added and continuously stirred for 48 h at room temperature. The obtained black colour product was separated by centrifugation

and washed with deionized water and ethanol for three times and dried in vacuum at 60 ºC overnight. The final product was denoted as MPDA framework.

2.4. Characterization

Morphologies of the sample were observed with a FEI Quanta FEG 200 scanning electron microscope (SEM) and with an accelerating voltage of 20 kV. High resolution transmission electron microscopy (HRTEM) images were obtained from JEOL, JEM, Fb-2000 instrument. The X-ray diffraction (XRD) was carried out on a PAN analytical, the Netherlands with Cu Ka radiation (λ=1.54 Å) at a voltage of 40 kV. The Fourier transform infrared spectroscopy (FT-IR) spectra were performed using an Agilent Technologies FT-IR spectrometer (USA). A model Fluoromax-4 Spectrofluorometer (HORIBA scientific, France) was used to record fluorescence emission spectra, with excitation and emission slit width of 10 nm. The samples were measured by excitation and emission wavelength was 490 nm and 520 nm. All the spectrophotometric of the hybrid material were performed with a suspension of sample dispersed in deionized water and then brought into quartz tube for measurement.

2.5. Procedure for Hg^{2+} detection

The detailed procedure for detection of Hg^{2+} as followed. First, the incorporated reaction was performed by mixing 50 nM FAM-labeled T-rich ssDNA probes (P-T DNA) and desired concentration of Hg^{2+} solution. Then, 20 units Exo III and Tris buffer solution was added to the solution, and the mixture was incubated at room temperature for 5 mins. Subsequently, the homogeneous mixture of the whole 200 μL solution was incubated at 37 ºC for 10 mins, where the activity of Exo III was completed at 75 ºC for 10 mins. Finally, the solution was cooled at room temperature, and then 10 μL as obtained MPDA framework stock solution was added to

the reaction solution, further incubated at room temperature for 10 mins. The fluorescence spectra were measured by different samples at excitation and emission wavelength of 490 nm and 520 nm respectively.

2.6. Procedure for Ag^+ detection

Similar to the above procedure, detection of Ag^+ also obtained. 50 nM FAM-labeled C-rich ssDNA probes (P- C DNA) and different concentrations of Ag^+ were mixed and the mixture was incubated for 5 mins at room temperature. Then, 20 units of Exo III were added and the whole solution was mixed homogeneously. After homogeneous mixing, the solution was incubated at 37 ºC for 30 mins and the activity of Exo III was completed by heating at 75 ºC for 10 mins. After that, the solution was slowly cooled at room temperature. Next, 10 µL (0.08 mg/mL) MPDA was added into above solution and incubated at room temperature for 10 mins. The fluorescence spectra were measured by different samples at excitation and emission wavelength of 490 nm and 520 nm respectively.

2.7. Analysis of real water samples

For the quantitative analysis of Hg^{2+} and Ag^+ in real water samples, a standard addition method was followed. The different mercury and silver containing water samples were collected from various places. Tap water was obtained from our laboratory. River water was taken from the Tamirabarani River (Tirunelveli, India). The samples were filtered from 0.22 µM membrane and all impurities were removed. For recovery studies, spiked with different concentration of mercury and silver were added to the samples and analyzed separately.

3. RESULTS AND DISCUSSION

3.1. Characterization

The ZIF-67 framework was synthesized by mixing of $Co(NO_3)_2$ and 2-methylimidazole in methanol solution. After that, the hollow metal polydopamine frameworks (MPDA) formed from the single–step transformation reaction between the dopamine solution and suspension of ZIF-67 in a mixture solution of ethanol and water **(scheme 1)**. **Figure 1A** showed scanning electron microscope (SEM) image of ZIF-67 crystals is confirmed that rhombic dodecahedra shape. The transmission electron spectroscopy (TEM) images of metal polydopamine framework are shown in **Figure 1B, C**. The ZIF-67 structure can destabilize with water due to hydrophobic nature of ZIF-67 and releasing the Co^{2+} and 2-methylimidazole. After addition of dopamine or polydopamine it would adsorb on the outer surface on the ZIF-67, thin layer PDA is formed around the ZIF-67 and maintained the original polyhedron structure. When the interaction between the released Co^{2+} ions in the breaking of Co-2-mim bonds, they coordinate with PDA resulting in the formation of a hollow structure with PDA and Co-PDA layer. We observed that ZIF-67 transformed completely hollow metal polydopamine framework is confirmed that TEM images in **Figure. 1B, C.**

The XRD measurements of MPDA and ZIF-67 are shown in **Figure 1D**. The diffraction peaks of ZIF-67 crystals noted at 2θ = 7.45º, 10.39º, 12.75º, 14.52º, 16.63º, 17.95º, 22.46º, 24.45º and 26.64º can be attributed to the (002), (112), (022), (013), (222), (114), (233) and (134) planes, respectively. All diffraction peaks of ZIF- 67 structure is completely disappeared in MPDA, which confirmed by transformation of ZIF-67 to MPDA. Furthermore, the FT-IR spectra of ZIF-67 and MPDA are shown in **Figure 1E.** The broad absorption band at 3338 cm^{-1} encompasses the O-H and N-H stretching vibration in MPDA. The characteristics FT-IR peaks at 1590 cm^{-1}

and 420 cm^{-1} can be assigned to the C=N and Co-N stretching vibrations in ZIF-67. These peaks are almost disappearing after transformation of ZIF-67 to MPDA.

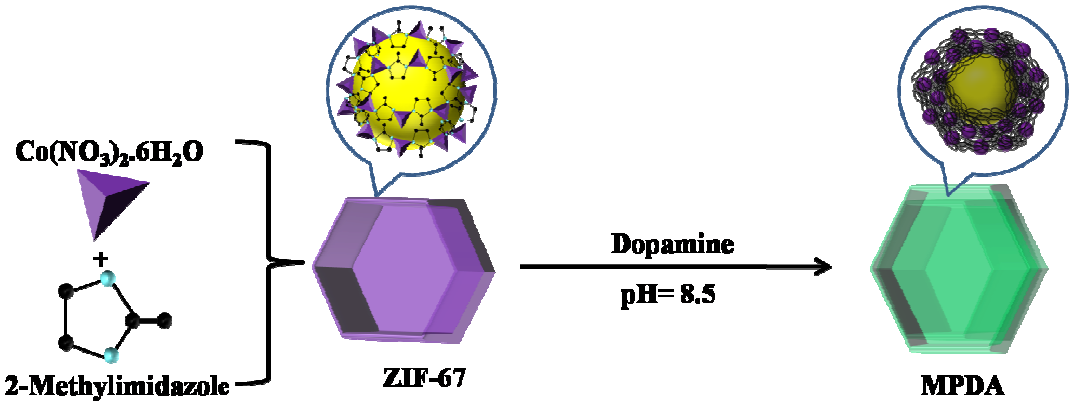

Scheme 1. Schematic illustration of the in-situ transformation from ZIF-67 into hollow Co-PDA polyhedral particles

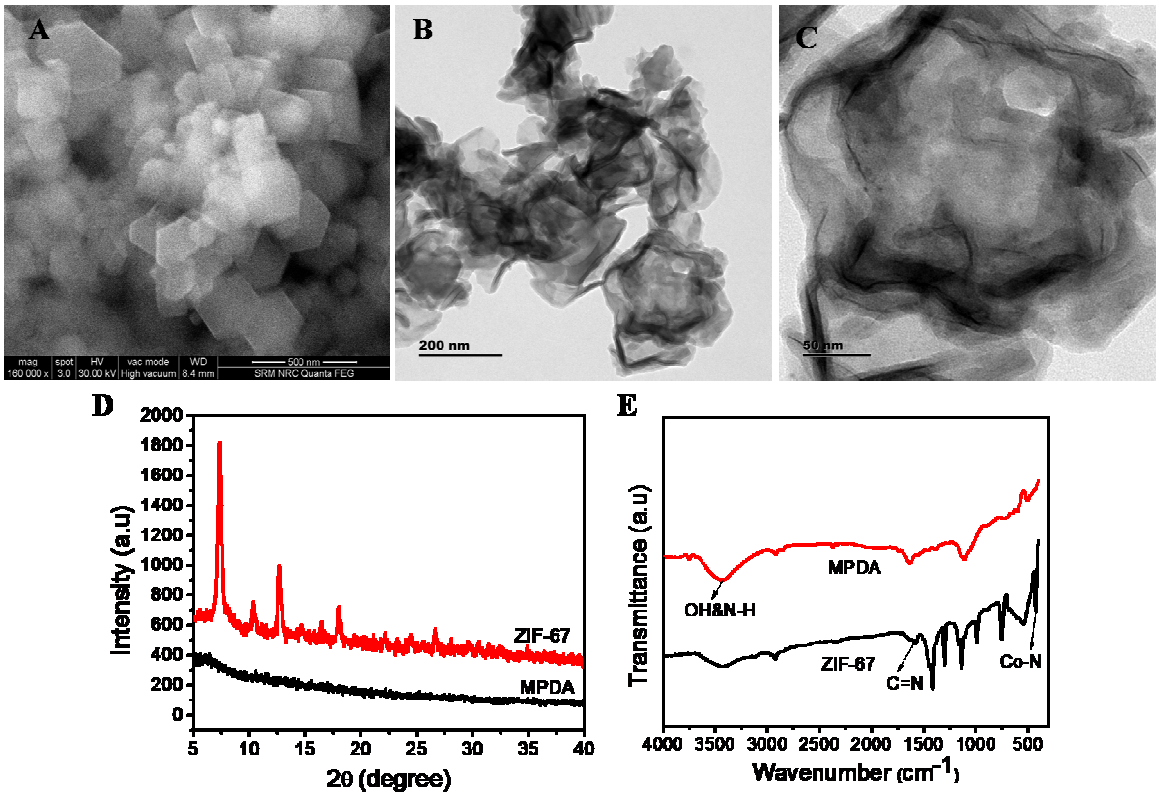

Figure 1. (A) SEM image of ZIF-67, (B, C) TEM images of MPDA, (D) XRD pattern of ZIF-67 and MPDA, (E) FT-IR spectra of ZIF-67 and MPDA.

3.2. Fluorescence quenching mechanism of MPDA

The fluorescence quenching ability of the metal polydopamine framework (MPDA) was shown in **Figure 2 A-D.** The sensing system of MPDA was consists of four types of ssDNA probes with attached different fluorophore including aminoethylcomarinacetate (AMCA), 6-carboxyfluorescein (FAM), carboxyteramethylrhodamine (TAMRA) and Cy5. In the absence of MPDA, the fluorophore attached ssDNA probes exhibited by strong fluorescence emission. Upon the addition of MPDA, which result in their strongly binding with fluorophore attached ssDNA probes and its fluorescence is quenched, obtainable different florescence emission signals at 450, 520, 575 and 660 nm respectively. The fluorescence quenching efficiency was calculated according to the formula QE= $(F_P\text{-}F_M/F_P) \times 100\%$, where F_P is the fluorescence intensity of the pure fluorophore attached ssDNAs and F_M is the fluorescence intensity of after addition of MPDA with fluorophore attached ssDNAs. The quenching efficiency of MPDA and four kinds of different fluorophore was reached up to above 97%. On the other hand, the 99.08% fluorescence quenching efficiency was achieved with the FAM labeled ssDNA probe. This phenomenon indicates that FAM-labeled ssDNA exhibits high fluorescence quenching efficiency compared to other fluorophore. The mechanism of interaction between the ssDNA and MPDA is related to the polydopamine nanospheres and nanotubes. The negatively charged phosphate backbone in ssDNA would adsorb on the surface of MPDA. The interaction of FAM labeled ssDNA on the surface of MPDA to the strong affinity by π-π stacking interaction between the exposed nucleobases and MPDA.[30] Moreover, the binding between FAM labeled ssDNA with MPDA may be happened due to the electrostatic and hydrogen bonding interaction between the nucleobases and aromatic groups of MPDA.[31] Moreover, we have made a comparison of MPDA with graphene oxide and metal oxides (Fe_3O_4, CeO_2) with fluorescence quenching performance,

displayed in **Figure 3A.** The FAM-labeled ssDNA was respectively mixed with same concentrations of MPDA, graphene oxide and metal oxides. It was found that MPDA has the highest quenching performance and lowest signal background fluorescence because polydopamine coordinated with Co^{2+} ion and formation of hollow metal-polydopamine frame work (MPDA) is obtained. The graphene oxide and metal oxides (Fe_3O_4, CeO_2) shows that less quenching performance compared to MPDA. The very less quenching performance activity of metal oxides compared with graphene oxide and MPDA is because of rigidity and reducing number of absorbing groups on surface.[32]

The UV-Vis spectrum of MPDA **(Figure 3B)** shows that the broad absorption spectra is overlapped with the emission spectra of fluorophores, So MPDA effectively quenches the fluorescence of those fluorophores due to FRET. Furthermore, the fluorescence life time of FAM labeled DNA is changed after the introduction of MPDA **(Figure 3C).** The above analysis provide strong evidence for the quenching of FAM labeled ssDNA and MPDA caused by the occasion of FRET. Based on the mechanism of fluorescence quenching of fluorophore via photo induced electron transfer (PET) and fluorescence resonance energy transfer (FRET). On the other hand, the Co^{2+} also participate the intrinsic fluorescent quenching property. So the quenching mechanism of MPDA may be PET.

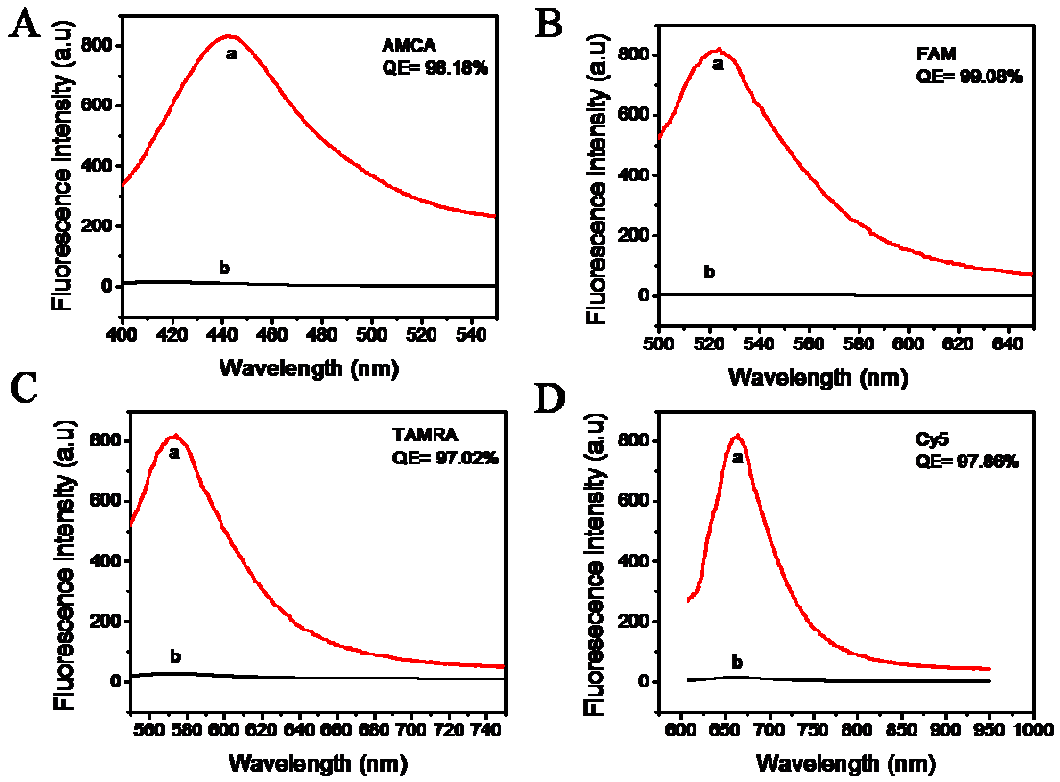

Figure 2. The fluorescence emission spectra of 50 nM of different fluorophores labeled probe DNA (A) Fluorescence emission spectra of AMCA labeled Probe DNA (a) Free AMCA labeled Probe DNA (b) AMCA labeled Probe DNA in presence of MPDA, (B) Fluorescence emission spectra of FAM labeled Probe DNA (a) Free FAM labeled Probe DNA (b) FAM labeled Probe DNA in presence of MPDA, (C) Fluorescence emission spectra of TAMRA labeled Probe DNA (a) Free TAMRA labeled Probe DNA (b) TAMRA labeled Probe DNA in presence of MPDA, (D) Fluorescence emission spectra of Cy5 labeled Probe DNA (a) Free Cy5 labeled Probe DNA (b) Cy5 labeled Probe DNA in presence of MPDA.

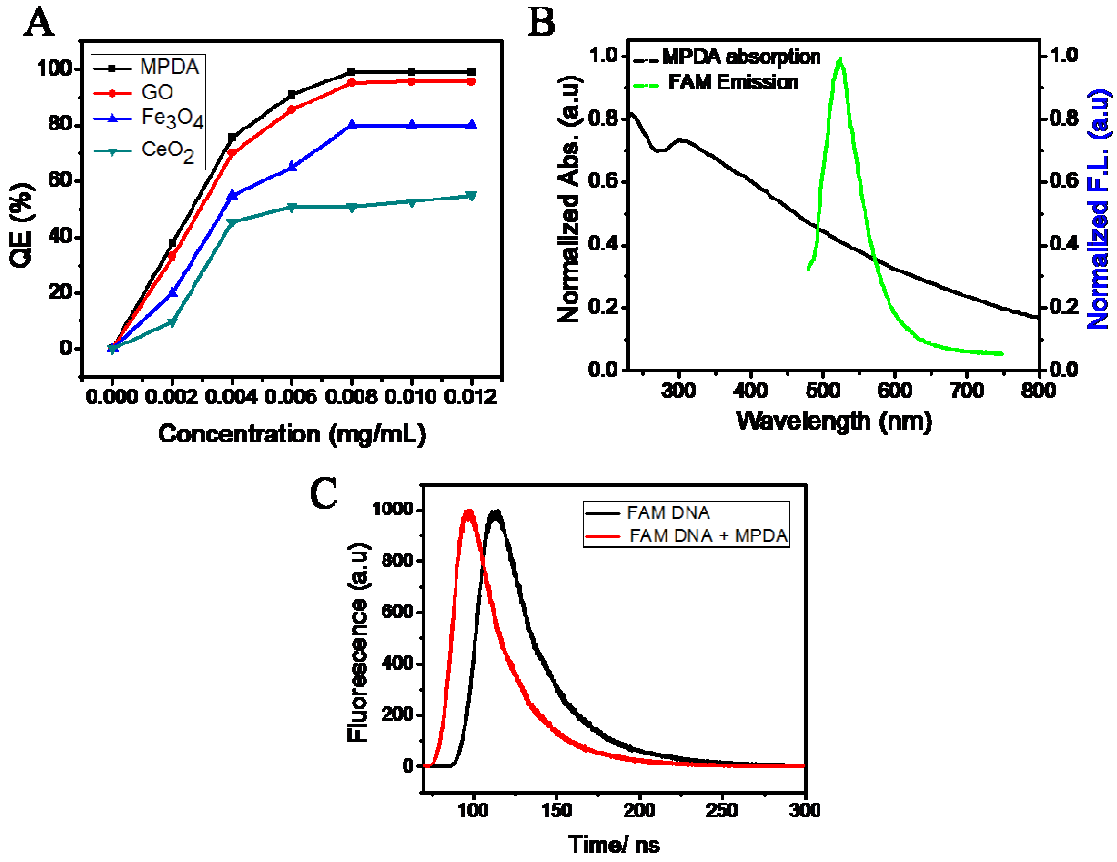

Figure 3. (A) Fluorescence quenching efficiency of different nanomaterials toward the 50 nM FAM labeled ssDNA with concentrations of nanomaterials (same concentrations of MPDA), (B) UV-Vis adsorption spectra of MPDA and emission spectra of FAM, (C) Fluorescence lifetime analysis of FAM labeled DNA, and after its adsorption by MPDA.

3.3. Optimization

The concentrations of MPDA used in this sensing system are considerable effect of different fluorescence quenching responses to the FAM-labeled ssDNA. Thus the fluorescence quenching efficiency of different concentrations of MPDA was investigated. As shown in **Figure 4A**, the fluorescence intensity at 520 nm of 50 nM of FAM-labeled ssDNA is gradually decreased with the increasing amount of MPDA. But, when the amount of MPDA was more than 0.08 mg/mL, the fluorescence intensity remains constant. So the 0.08 mg/mL was taken as the optimized

amount of MPDA. The adsorption and desorption kinetics behavior of FAM labeled ssDNA on MPDA have also been investigated by monitoring the changes in fluorescence intensity as function of time **(Figure 4C)**. The kinetics of fluorescence quenching reaction is quite fast. The $F\text{-}F_0/F_0$ values increased and fluorescence intensity is decreased within 5 min. However in presence of target metal ions, the $F\text{-}F_0/F_0$ values are decreased and fluorescence enhancement is gradually increased with increase of incubation time, reaching a saturated $F\text{-}F_0/F_0$ value in 10 min. We studied that absorbing and desorbing kinetics of FAM labeled ssDNA and MPDA and found that 5 min and 10 min were required for efficient sensing process.

The acidic medium of the solution have a notable influence of the fluorescence detection of Hg^{2+} and Ag^{+}. The pH value below 7, the Hg^{2+} and Ag^{+} has reduce the affinity of thymine and cytosine bases due to protonation of nitrogen atoms in bases. The fluorescence response is very poor at increasing pH above 7 because of the partial participation of hydroxide ions. Therefore, different pH values were optimized (**Figure 4D**). The $F\text{-}F_0/F_0$ (where F and F_0 values are presence and absence of target ions) values increased when the pH was 5-7.5. After increasing the pH of the solution the $F\text{-}F_0/F_0$ values are decreased. It concern that the performance of the sensing system is chosen for the optimized pH-7.5. Finally, the effect of amount of Exo III of the sensing system was investigated, which as shown in **Figure 4E**.The increasing amount of Exo III with increasing $F\text{-}F_0/F_0$ values and reached up to 20 units the $F\text{-}F_0/F_0$ values is constant. Therefore, 20 units Exo III was found to be optimum amount and further used.

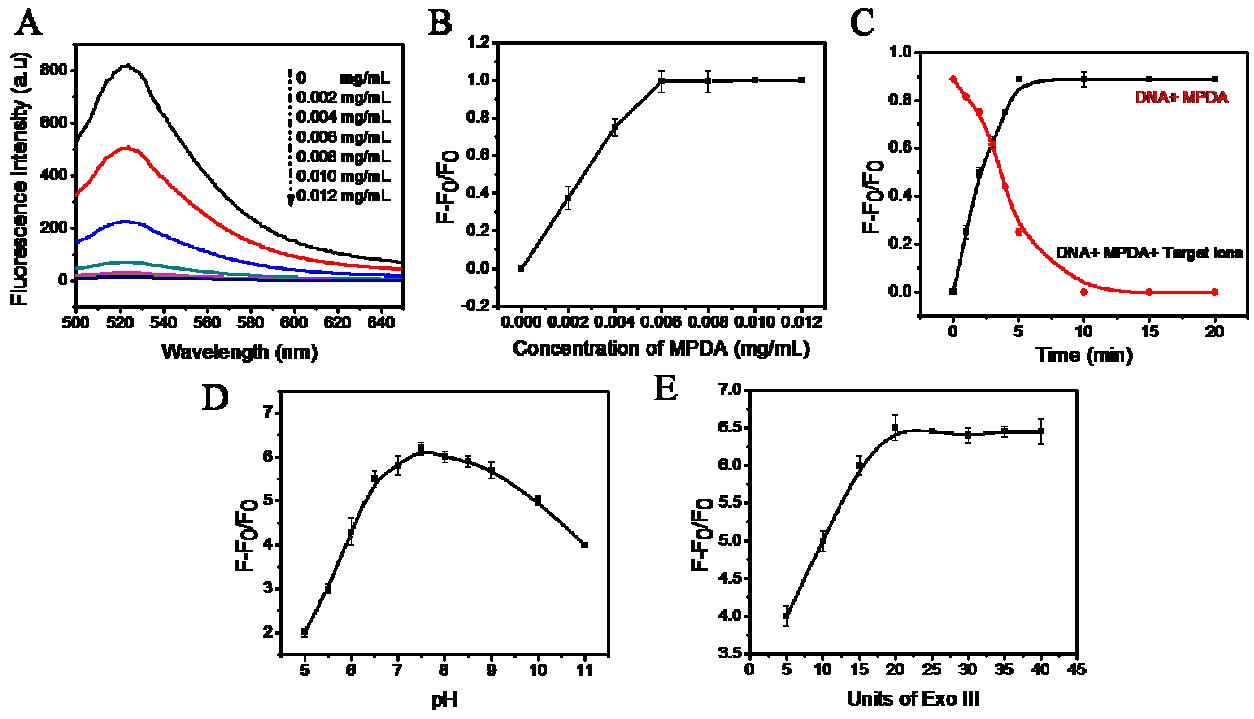

Figure 4. (A, B) The fluorescence emission spectra of 50 nM FAM labeled ssDNA with different amounts of MPDA, The optimization of (C) Time (D) pH and (E) amounts of Exo III. F is the fluorescence intensity of the presence of target ions and F_0 is absence of target ions respectively.

3.4. Sensitivity and selectivity of Hg^{2+} sensor

The metal-polydopamine frameworks (MPDA) acts as an efficient quencher for different fluorophore labeled ssDNA. More importantly, these frameworks are exhibit good adsorbed ssDNA and discriminate to the dsDNA. The Exonuclease III assisted target recycling method is widely used for the detection of Hg^{2+} ions. This method is very highly sensitive detection of Hg^{2+} ions compared to other without Exonuclease III assisted target recycling method. The T-rich ssDNA probes are interacts with Hg^{2+} and formation of T-Hg^{2+}-T base pairs in the dsDNA.[33] The Exo III is frequently used for the Exonuclease III assisted target recycling method and it could catalyze the stepwise removal of mononucleotides from 3' and 5' end of dsDNA.[34] The removal

of mononucleotides is not absorbed to the surface of MPDA due to less negative of mononucleotides. The liberating Hg^{2+} can undergo many T-Hg^{2+}-T base pairs to releasing the another ssDNA. These cyclic reactions are producing the amplification fluorescence signal and determine the very small quantity of Hg^{2+}. The MPDA and Exonuclease III assisted method is versatile platform for fluorescence detection of Hg^{2+} is displayed in **scheme 2.** To validate the feasibility study of detection of Hg^{2+} is shown in **Figure 5A**. In the presence of FAM labeled ssDNA and MPDA, the fluorescence intensity is completely quenched by MPDA and addition of Exo III slightly changes in the fluorescence intensity (curve a, b). And in presence of Hg^{2+}, the FAM labeled T-rich ssDNA probes and MPDA system the fluorescence intensity is partially increased due to formation of T-Hg^{2+}-T base pairs in the dsDNA (Curve c). After the addition of Exo III, the fluorescence intensity dramatically increased (curve d). Under optimized conditions, different concentrations of Hg^{2+} were performed in this sensing system. The concentration of Hg^{2+} increased with increasing the fluorescence intensity at the concentration of 0 to 350 nM (**Figure 5B**). The fluorescence intensity is clearly shows that gradually increased from lower to higher concentration of Hg^{2+}. **Figure 5C** depicts the relative fluorescent intensity plotted against Hg^{2+} concentration. The linear relationship between the concentrations of Hg^{2+} and fluorescence intensity ranging from 0-2 nM and correlation coefficient value R^2= 0.989 (**Figure 5D**). The limit of detection was achieved from 1.3 pM according to the 3σ method. The detection limit of this biosensing system is lower than the other sensing system (**Table 1**). The selectivity of this sensing was also investigated.

The interfering metal ions such as Ni^{2+}, Zn^{2+}, Fe^{3+}, Cu^{2+}, Ca^{2+}, Pb^{2+}, Co^{2+} and Cd^{2+} with mixing of Hg^{2+} at concentration of 5μM and 100 nM. The fluorescence intensity of interfering metal ions is negligible. However, the fluorescence intensity of Hg^{2+} is high due to formation of T-Hg^{2+}-T base pairs (**Figure 5E**). So this result indicates that Hg^{2+} is high specificity of this sensing platform.

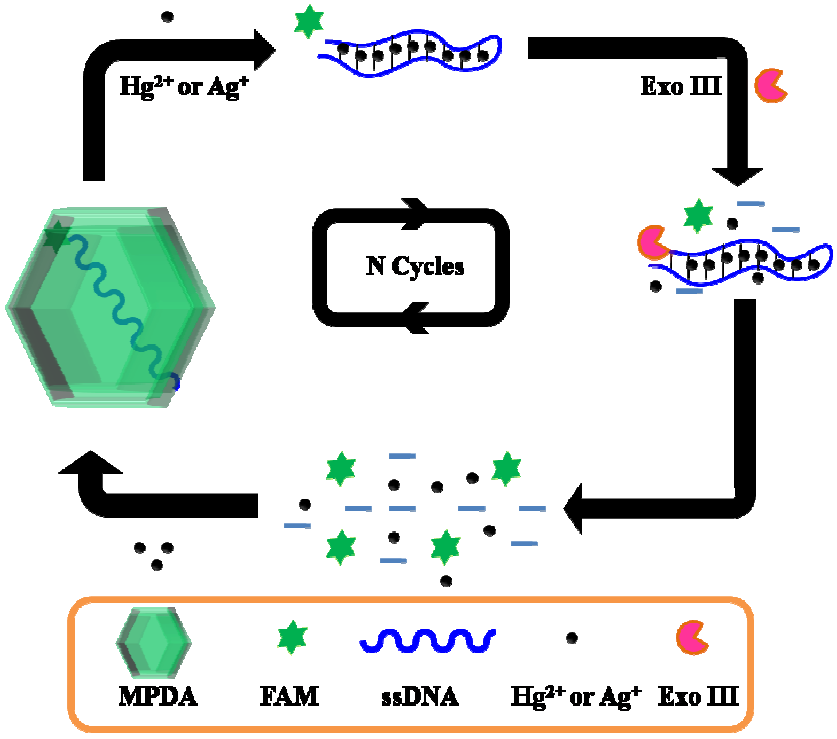

Scheme 2. Schematic illustration for MPDA based fluorescent sensing system for the detection of Hg^{2+} and Ag^{+} assisted Exonuclease III amplification.

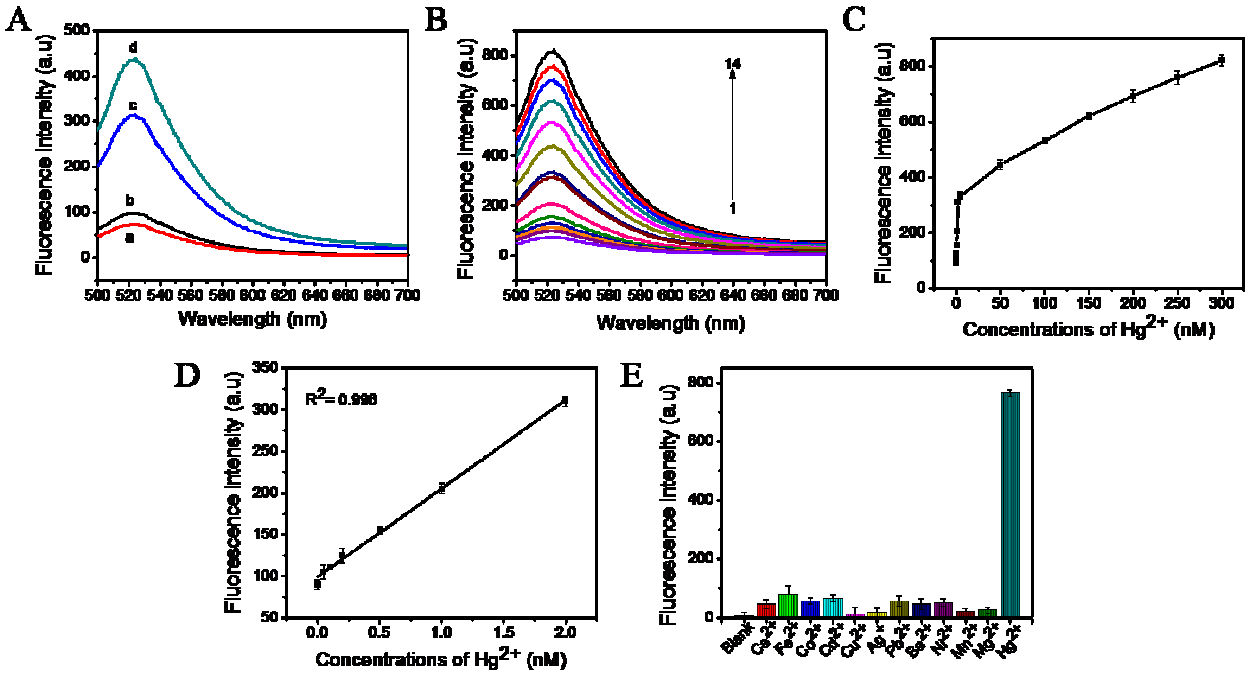

Figure 5. (A) The fluorescence spectra of (a) 50 nM of FAM labeled ssDNA with MPDA, (b) 50 nM of FAM labeled ssDNA and MPDA with 20 U Exo III, (c)) 50 nM of FAM labeled ssDNA and MPDA with 100 nM of Hg^{2+}, (d) 50 nM of FAM labeled ssDNA, MPDA, 100 nM of Hg^{2+} and 20 U Exo III, (B) The fluorescence emission spectra of 50 nM of FAM labeled ssDNA and MPDA with different concentrations of Hg^{2+}, (C) The fluorescence intensity verses concentrations of Hg^{2+}, (D) The linear relationship between the fluorescence intensity and concentrations of Hg^{2+}, (E) The fluorescence spectra of different metal ions with Hg^{2+}.

Table 1. Comparisons of different nanomaterials for mercury determination.

Materials[a]	Method[b]	LOD[c]	Real sample	Ref
MPDA/Exo III	F	1.2 pM	Tap and river water	Present work
2-Aminopurine /DNA	F	3 nM	Lake water	36
ssDNA/AgNCs	F	4.5 nM	Lake and Tap water	37
T-rich DNA/NGO	F	8.5 nM	Not reported	38
GO/DNAzyme/ThT	F	356 pM	Tap and lake water	13
ssDNA/WS_2	F	3.3 nM	Tap water	18
Exo III/ GO	F	0.3 nM	Tap and river water	19
AuNPs/DNA	F	16 nM	River water	39
g-C_3N_4/ssDNA	F	0.17 nM	Tap water	40
Ag@SiO_2	F	0.33 nM	Not reported	41

[a]AgNCs, Silver nanoclusters; NGO, nano-sized graphene oxide; GO, graphene oxide; ThT, Thioflavin T; WS_2, Tungsten disulfide; Exo III, exonuclease III; g-C_3N_4, graphite carbon nitride; [b]F , fluorescence; [c]LOD, limit of detection.

3.5. Sensitivity and selectivity of Ag^+ sensor

To explore the mechanism of MPDA based fluorescence detection of Ag^+ assisted Exo III amplification method. The FAM labeled C-rich ssDNA probes is adsorbed on the surface of MPDA and fluorescence intensity is completely quenched. After the addition of Ag^+, the FAM labeled C-rich ssDNA probes is self hybridized and to form C-Ag^+-C base pairs[35] with respective dsDNA. The interaction between the dsDNA and surface of MPDA is very weak. The well folded and stable dsDNA by C-Ag^+-C base pairs can be digested by after the addition of Exo III and releasing the many mononucleotides. These mononucleotides does not adsorb on the surface

of MPDA so fluorescence intensity dramatically increased. The above a mentioned mechanism of this sensing system was performed on the detection of Ag^+ (**scheme 2**). First, the feasibility study for detection of Ag^+ as shown in **Figure 6A.** The fluorescence intensity completely quenched was caused by FAM labeled C-rich ssDNA probes absorbed on the surface of MPDA (Curve a). The non-negligible fluorescence intensity was observed in the presence of Exo III (Curve b), revealing that Exo III is not specifying the digests of ssDNA. However, the addition of Ag^+ the very weak fluorescence intensity showed due to most of the FAM labeled C-rich ssDNA probes adsorbed on the MPDA (Curve C) and addition of Exo III the fluorescence intensity dramatically increased because the Exo III was digested by the dsDNA (Curve d). The Quantitative determination of Ag^+ was carried under optimized conditions. As shown in **Figure 6B**, with increasing concentrations of Ag^+ (0-300 nM), the fluorescence intensity is increased gradually. **Figure. 6C** presents the relationship between the fluorescence intensity and concentrations of Ag^+. The linear relationship between the fluorescence intensity at 520 nm and the concentrations of Ag^+ in the range of 1-3 nM with a detection limit of 34 pM is calculated from according to the 3σ method (**Figure 6D**). The detection limit was compared with other reports (**Table 2**).

The selectivity of Ag^+ sensing system was also evaluated by monitoring fluorescence response when the sensing system challenged other metal ion. To confirm the selectivity of Ag^+ sensor , other different metal ions including Ni^{2+}, Zn^{2+}, Fe^{3+}, Cu^{2+}, Ca^{2+}, Pb^{2+}, Co^{2+} and Cd^{2+} with the same concentration of 5 μM is 10 time greater than target metal Ag^+ and response of the fluorescence sensor is depicted in **Figure 6E**. As shown in the figure, it was clearly shows that no significant fluorescence responses with addition of other metal ions except Ag^+. These results indicate that this sensing system had excellent selectivity of Ag^+ compared to other metal ions.

The high selectivity of this sensing system is due to the fact that C-Ag^+-C mismatch shows high affinity for Ag^+ against other metal ions.

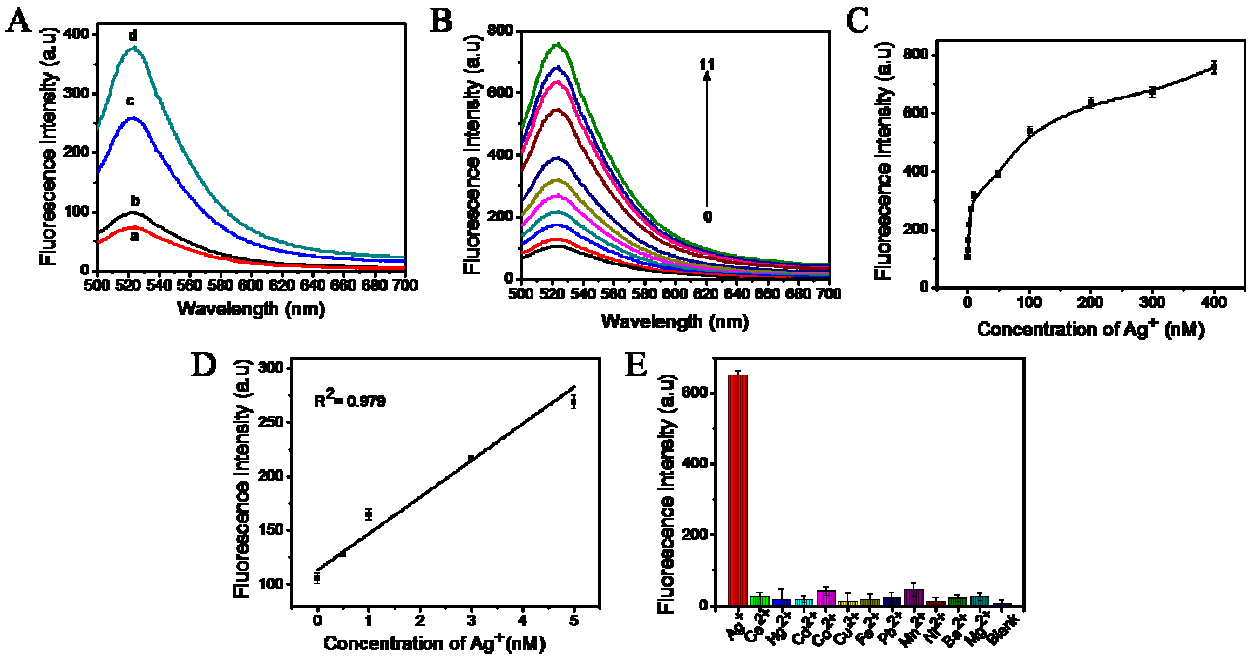

Figure 6. (A) The fluorescence spectra of (a) 50 nM of FAM labeled ssDNA with MPDA, (b) 50 nM of FAM labeled ssDNA and MPDA with 20 U Exo III, (c)) 50 nM of FAM labeled ssDNA and MPDA with 100 nM of Ag^+, (d) 50 nM of FAM labeled ssDNA, MPDA, 100 nM of Ag^+ and 20 U Exo III, (B) The fluorescence emission spectra of 50 nM of FAM labeled ssDNA and MPDA with different concentrations of Ag^+, (C) The fluorescence intensity verses concentrations of Ag^+, (D) The linear relationship between the fluorescence intensity and concentrations of Ag^+, (E) The fluorescence spectra of different metal ions with Ag^+.

Table 2. Comparison of different nanomaterials for silver determination.

Materials[a]	Method[b]	LOD[c]	Real sample	Ref
MPDA/Exo III	F	34 pM	Tap and river water	Present work
2-Aminopurine /DNA	F	3 nM	Lake water	36
ssDNA/WS_2	F	1.2 nM	Tap water	18
Exo III/ GO	F	0.1 nM	Lake water	35
SYBER Green	F	4.3 nM	Not reported	42
QDs/Ru complex/CNTs	F	0.1 μM	Not reported	43
GO	F	5 nM	River water	44
Bifunctional SDA	F	16 pM	Tap water	45

[a]WS_2, Tungsten disulfide; GO, graphene oxide; Exo III, exonuclease III; QDs, Quantum dots; CNTs, carbon nanotubes; [b]F , fluorescence; [c]LOD, limit of detection.

3.6. Analysis of the real water samples

To further evaluate the potential application of the sensing system to detect trace amount of Hg^{2+} and Ag^{+} in different environmental water samples. The collected real water samples including tap and river water were analyzed using the MPDA with assisted Exo III amplification sensing system. The desired amount of Hg^{2+} and Ag^{+} was spiked with different concentrations (10, 20, 30 nM) into water samples followed by the addition of the MPDA sensor to each samples. In this experiment carried out a normal detection process was carried out with three replicates. The obtained results are summarized in **Table 3** with satisfactory results between the 95-105% were taken in the recovery experiments. To prove the reliability by the our sensor (MPDA) with Exo III assisted amplification sensing system had potential for assaying Hg^{2+} and Ag^{+} ions in environmental water samples.

Table 3. Recoveries for the determination of Hg^{2+} and Ag^{+} ions in real water samples

Sample	Spiked (nM)	Detected ±SD		Recovery (%)	
		Hg^{2+}	Ag^{+}	Hg^{2+}	Ag^{+}
Tap water	0	N.D	N.D	-	-
	10	$10.01^{a} \pm 0.45^{b}$	$9.65^{a} \pm 0.55^{b}$	100.1	96.5
	20	$20.26^{a} \pm 0.21^{b}$	$19.26^{a} \pm 0.66^{b}$	101.3	96.3
	30	$29.79^{a} \pm 1.2^{b}$	$30.03^{a} \pm 2.4^{b}$	99.3	100.1
River water	0	N.D	N.D	-	-
	10	$10.05^{a} \pm 0.23^{b}$	$10.09^{a} \pm 0.76^{b}$	100.5	100.9
	20	$19.79^{a} \pm 0.15^{b}$	$19.56^{a} \pm 0.10^{b}$	98.95	97.8
	30	$29.22^{a} \pm 0.18^{b}$	$30.22^{a} \pm 0.28^{b}$	97.4	100.73

4. CONCLUSION

In summary, this work developed a metal polydopamine framework (MPDA) applied to the study of the fluorescence quenching abilities of various fluorescent dyes such as aminoethylcomarin acetate (AMCA), 6-carboxyfluorescein (FAM), carboxyteramethylrhodamine (TAMRA) and Cy5 used as a versatile sensing platform for detection of Hg^{2+} and Ag^{+} was achieved for the first time. The resultant (MPDA) sensor also has an outstanding sensitive and selective detection of Hg^{2+} and Ag^{+} ions through Exo III assisted signal amplification. The detection limit of Hg^{2+} and Ag^{+} was found to be 1.2 pM and 34 pM respectively, which was superior to that of the previously reported sensing systems. Additionally,

the detection limit is much lower than the EPA and WHO limit of Hg^{2+} & Ag^{+} ions in drinkable water. Furthermore, this sensing system was successfully demonstrated for the analysis of Hg^{2+} and Ag^{+} with satisfactory recovery results. This, in turn, facilitates the development and utilization of this sensing platform and it can be generally applied for various applications including other detection of heavy metals and biomolecules.

Acknowledgements

Author acknowledges the financial support from the Department of Chemistry, SRM Institute of Science and Technology, Tamil Nadu - 603 203, India.

REFERENCES

1. Wang, G.; Xu, G.; Zhu, Y.; Zhang, X. A 'turn on" carbon nanotube–Ag nanoclusters fluorescent sensor for sensitive and selective detection of Hg^{2+} with cyclic amplification of exonuclease III activity. *Chem. Commun.* **2014**, 50, 747-750.
2. Ke, J.; Li, X.; Zhao. Q.; Hou, Y.; Chen, J. Ultrasensitive quantum dot fluorescence quenching assay for selective detection of mercury ions in drinking water. *Sci. Rep.* **2014**, 4, 5624.
3. Barriada, J. L.; Tappin, A. D. Evans, E. H.; Achterberg, E. P. Dissolved silver measurements in seawater. *TrAC, trends anal. Chem*. 2007, 26(8), 809-817.
4. Ratte, H. T. Bioaccumulation and toxicity of silver compounds: review. *Environ Toxicol Chem.* **1999**, 18, 89-108.

5. Huang, J.; Gao, X.; Jia, J.; Kim, J. K.; Li. Z. Graphene oxide-based amplified fluorescent biosensor for Hg^{2+} detection through hybridization chain reactions. *Anal. Chem.* **2014**, 86, 3209-3215.
6. Guo, Z. Q.; Zhu, W. H.; Tian, H. Dicyanomethylene-4*H*-pyran chromophores for OLED emitters, logic gates and optical chemosensors. *Chem. Commun*. **2012**, 48, 6073-6076.
7. Lin, Z. H.; Zhu, G.; Zhou, Y. S.; Yang, Z.; Bai. P.; Chen, J.; Wang, Z. L. A self-powered triboelectric nanosensor for mercury ion detection. Angew. Chem. Int. Ed. **2013**, 52, 5065-5069.
8. Pu, Q.; Sun, Q. Application of 2-mercaptobenzothiozole-modified silica gel to on-line preconcentration and separation of silver for its atomic adsorption spectrometric determination. *Analyst*, **1998**, 123, 239.
9. Li. Y.; Chen, C.; Li. B.; Sun, J.; Wang, J.; Gao, Y.; Zhao, Z.; Chai, Z. Elimination efficiency of different reagents for the memory effect of mercury using ICP-MS. *J.Anal.at. spectrom.* **2006**, 21, 94-96.
10. Krachler, M.; Mohl, C.; Emons, H.; Shotyk, W. Analytical procedures for the determination of selected trace elements in peat and plant samples by inductively coupled plasma mass spectrometry. *Spectrochem. Acta. Part B.* **2002**, 57, 1277-1289.
11. Aranda, P. R.; Pacheco, P. H.; Olsina, R. A.; Martinez, L. D.; Gil, R. A. Total and inorganic mercury determination in biodiesel by emulsion sample introduction and FI-CV-AFS after multivariate optimization. *J.Anal.at. spectrom.* **2009**, 24, 1441-1445.
12. Yang, x. J.; Foley, R.; Low, G. K. C. A modified digestion procedure for analyzing silver in environmental water samples. *Analyst*, **2002**, 127, 315-318.

13. Ravikumar, A.; Panneerselvam, P.; Radhakrishnan, K. Fluorometric determination of lead(II) and mercury(II) based on their interaction with a complex formed between graphene oxide and a DNAzyme. *Microchim Acta,* **2018**, 2, 182.

14. Saran, R.; Liu, J. A Silver DNAzyme. *Anal. Chem.* **2016**, 88(7), 4014-4020.

15. Zhang, S.; Zhang, D.; Zhnag, X.; Shang, D.; Xue, Z.; Shan, D.; Quan Lu, X. Ultratrace naked-eye colorimetric detection o Hg in wastewater and serum utilizing mercury-stimulated peroxidase mimetic activity of reduced graphene oxide-PEI-Pd nanohybrides. *Anal. Chem.* **2017**, 89(6), 3538-3544.

16. Li. B.; Du, Y.; Dong. S. DNA based gold nanoparticles colorimetric sensors for sensitive and selective detection of Ag(I) ions. *Anal. Chim. Acta.* **2009**, 644, 78-82.

17. Zhang, Y.; Zeng, G. M.; Tang, L.; Li, Y. P.; Chen, Z. M.; Huang, G. H. Quantitative detection of trace mercury in environmental media using a three-dimensional electrochemical sensor with a anionic intercalator. *RSC. Adv*. **2014**, 18485 -18492.

18. Zuo, X.; Zhang, H.; Zhu, Q.; Wang, W.; Feng, J.; Chen, X. A dual-color fluorescent biosensing platform based on WS_2 nanosheet for detection of Hg^{2+} and Ag^{+}. Biosens. Bioelectron. **2016**, 85, 464-470.

19. Zhang, Y.; Tang, T.; Yang, F.; Sun, Z.; Zhang, G. J.; Highly sensitive DNA-based fluorometric mercury(II) bioassay based on graphene oxide and exonuclease III- assisted signal amplification. *Microchim Acta.* **2015**, 182, 1535-1541.

20. Wang, Q.; Wang, W.; Lei, J.; Xu, N.; Gao, F.; Ju, H.; Fluorescence quenching of carbon nitride nanosheet through its interaction with DNA for versatile fluorescence sensing. *Anal.chem.* **2013**, 85, 12182-12188.

21. Mao, K.; Wu, Z.; Chen, Y.; Zhou, X.; Shen, A.; Hu, J. A novel biosensor based on single-layer MoS_2 nanosheets for detection of Ag^+. *Talanta*, **2015**, 132, 658-663.

22. Niu, S. Y.; Li, Q. Y.; Ren, R.; Hu, K. C. DNA/single–walled carbon nanotubes based fluorescent detection of Hg^{2+}. *Anal. Lett.* **2010**, 43(15), 2432-2439.

23. Fang, J. M.; Leng, F.; Zhao, X. J.; Hu, X. L.; Li, Y. F. Metal-organic framework MIL-101 as a low background signal platform for label-free DNA detection. *Analyst*, **2014**, 139, 801-806.

24. Karthick, P.; Pandikumar, A.; Preeyanghaa, M.; Kowsalya, M.; Neppolian, B. Amino-functionalized MIL-101(Fe) metal-organic framework as a viable fluorescent probe for nitro aromatic compounds. *Microchim. Acta*. **2017**, 184(7), 2265-2273.

25. Fan, D.; Zhu, X.; Zhai, Q.; Wang, E.; Dong, S. Polydopamine nanotubes as an efficient fluorescent quencher for highly sensitive and selective detection of biomolecules assisted with exonuclease III amplification. *Anal. Chem.* **2016**, 88(18), 9158-9165.

26. Liu. Y.; Ai, K.; Lu, L.; Polydopamine and its derivative materials: Synthesis and promising applications in energy, environmental, and biomedical fields. *Chem. Rev.* **2014**, 114, 5057-5115.

27. Ji, X.; Palui, G.; Avellini, T.; Na, H. B.; Yi, C. Y.; Jr, K. L. K.; Mattoussi, H. On the pH-dependent quenching of quantum dot photoluminescence by redox active dopamine. J. Am. Chem. Soc. **2012**, 134, 6006-6017.

28. Yanna, G.; Jing, T.; Huayu, Q.; Zhingli, W.; Yusuke, Y. One-pot synthesis of zeolitic imidazolate framework 67-derived hollow Co_3S_4@MoS_2 heterostrutures as efficient bifuntional catalysts, Chem. Mater. **2017**, 29, 5566-5573.

29. Liang, Y.; Wei, J.; Hu, Y. X.; Chen, X. F.; Zhang, J.; Zhang, X. Y.; Jiang, S. P.; Tao, S. W.; Wang, H. T.; Metal-polydopamine frameworks and their transformation to hollow metal/N-doped carbon particles. *Nanoscale*, **2017**, 9, 5323-5328.

30. Zhou, W.; Saran, R.; Liu, J.; Metal sensing by DNA. **2017**, 117, 8272-8325.

31. Zhou, Y.; Huang, Z.; Yang, R.; Liu, J.; Slection and screening of apatamers for inorganic nanomaterials. Chem.- Eur.J. **2018**, 24, 2525-2532.

32. Liu, B.; Ma, L.; Huang, Z.; Hu, H.; Wu, Liu, J.; Janus DNA orthogonal adsorption of graphene oxide and metal oxide nanoparticles enabling stable sensing in serum. Mater. Horiz. **2018**, 5, 65-69.

33. Huang, J.; Gao, X.; Jia, J.; Kim, J. K.; Li, Z. Graphene oxide-based amplified fluorescent biosensor for Hg^{2+} detection through hybridization chain reactions, *Anal. Chem.* **2014**, 86, 3209-3215.

34. Xi, Q.; Zhou, D. M.; Kan, Y. Y.; Ge, J.; Wu, z. K.; Yu, R. Q.; Jiang, J. H. Highly sensitive and selective streategy for MicroRNA detection based on WS_2 nanosheet mediated fluorescence quenching and duplex-specific nuclease signal amplification. *Anal. Chem.* **2014**, 86, 1361-1365. `

35. Lang, M.; Li, Q.; Huang, H.; Yu, F.; Chen, Q. Highly sensitive exonuclease III-assisted fluorometric determination of silver(I) based on graphene oxide and self-hybridization of cytosine-rich ss-DNA. *Microchim Acta.* **2016**, 183, 1659-1665.

36. Zhou, W.; Ding, J.; Liu, J. 2-Aminopurine-modified DNA homopolymers for robust and sensitive detection of mercury and silver. *Biosens. Bioelectron*. **2017**, 87, 171-177.

37. Li, C.; Wei, C. DNA-templated silver nanocluster as a label-free fluorescent probe for the highly sensitive and selective detection of mercury ions, Sens. and Actuators: B chemical. **2017**, 242, 563-568.

38. Huang, P. P. J.; Ballegooie, C. V.; Liu, J.; Hg^{2+} detection using a phosphorothioate RNA probe adsorbed on graphene oxide and a comparison with thymine-rich DNA. *Analyst*, **2016**, 141, 3788-3793.

39. Tan, D.; He, Y.; Xing, X.; Zhao, Y.; Tang, H.; Pang, D. Aptamer functionalized gold nanoparticles based fluorescent probe for the detection of mercury (II) ion in aqueous solution. *Talanta,* **2013**, 113, 26-30.

40. Li, J.; Wang, H.; Guo, Z.; Wang, Y.; Ma, H.; Ren, X.; Du, B.; Wei, Q. A "turn-off" fluorescent biosensor for the detection of mercury (II) based on graphite carbon nitride. *Talanta,* **2017**, 162, 46-51.

41. Pang, Y.; Rong, Z.; Xiao, R.; Wang, S.; "Turn on " and label-free core-shell $Ag@SiO_2$ nanoparticles-based metal-enhanced fluorescent (MEF) aptasensor for Hg^{2+}, Sci. reports, **2015**, 5, 9451.

42. Pu, W. D.; Zhao, H. W.; Huang, C. Z.; Wu, L. P.; Xua, D. Fluorescent detection of silver (I) and cysteine using SYBER Green I and silver (I)- specific oligonucleotide. *Microchim Acta,* **2012**, 177, 137 -144.

43. Sun, W.; Yao, J.; Yao, T.; Shi, S. Label-free fluorescent DNA sensor for the detection of silver ions based on molecular light switch Ru complex and unmodified quantum dots, *Analyst,* **2013**, 138, 421-424.

44. Wen, Y.; Xing, F.; He, S.; Song, S.; Wang, L.; Long, Y.; Li, D.; Fan, C. A graphene-based fluorescent nanoprobe for silver (I) ions detection by using graphene oxide and a silver-specific oligonucleotides. *Chem. Commun.* **2010**, 46, 2596-2598.

45. Zhu, G.; Li, Y.; Zhang, C. Y.; Simultaneous detection of mercury(II) and silver(I) ions with picomolar sensitivity. *Chem. Commun.* **2010**, 50, 572-574.

FOR TOC ONLY